

The GL 569 Multiple System

M. SIMON¹, C. BENDER¹, AND L. PRATO²

ABSTRACT

We report the results of high spectral and angular resolution infrared observations of the multiple system GL 569 A and B that were intended to measure the dynamical masses of the brown dwarf binary believed to comprise GL 569 B. Our analysis did not yield this result but, instead, revealed two surprises. First, at age ~ 100 Myr, the system is younger than had been reported earlier. Second, our spectroscopic and photometric results provide support for earlier indications that GL 569 B is actually a hierarchical brown dwarf triple rather than a binary. Our results suggest that the three components of GL 569 B have roughly equal mass, $\sim 0.04 M_{\odot}$.

Subject headings: stars: binaries: visual — binaries: spectroscopic — stars: low-mass, brown dwarfs — stars: pre-main sequence — techniques: high angular resolution — techniques: radial velocities

1. INTRODUCTION

Accurate and precise measurements of the masses of brown dwarfs are necessary to validate the theoretical calculations of their evolution and to determine their location in the HR diagram (Burrows et al. 1997; Baraffe et al. 2003). Astrometric and spectroscopic observations of binaries provide the means to accomplish this dynamically. When the distance to the binary is known, the astrometric orbit of an angularly resolved binary (hence a “visual binary”, VB) determines the total mass, M_{tot} . A double-lined spectroscopic binary (SB2) provides the mass ratio. When a binary can be observed as both a VB and SB2, the component masses can be determined. Since the VB also yields the orbital inclination, the VB and SB2 measurements together provide an independent determination of the binary’s distance. In the special case of an eclipsing binary, the orbital inclination is $\sim \pi/2$ and the SB2 observations alone suffice to determine the component masses.

¹Department of Physics and Astronomy, SUNY, Stony Brook, NY 11794-3800

²Lowell Observatory, 1400 West Mars Hill Rd. Flagstaff, AZ 86001

Although brown dwarf binaries are not rare (Burgasser et al. 2005), precise dynamical masses are known only for the brown dwarf components of the eclipsing binary in Orion discovered by Stassun et al. (2005). Their masses, radii, and effective temperatures agree reasonably well with the models, but surprisingly, the effective temperature of the primary is found to be cooler than that of the secondary. Zapatero Osorio et al. (2004), Bouy et al. (2004), and Pravdo et al. (2005) have reported brown dwarf masses based on an astrometrically determined M_{tot} and photometry, but reliable masses determined dynamically are not yet available. Zapatero Osorio et al. (2004) obtained angularly resolved spectra of GL 569 Ba and Bb but their measurements were insufficient to yield dynamical masses. Because only two brown dwarf masses are known, and they raise a puzzle that requires confirmation, it is desirable to enlarge the sample of dynamically determined masses and to cover as large a range of mass and age as possible.

GL 569 is a multiple system comprised of GL 569 A, a M2.5V star (Henry & Kirkpatrick 1990) of mass $M = 0.35 \pm 0.03 M_{\odot}$ (Gorlova et al. 2003) at the *HIPPARCOS* distance 9.81 ± 0.16 pc, and GL 569 B, thought to be a binary brown dwarf with period ~ 876 days (Zapatero Osorio et al. 2004). We began a study of GL 569 B in 2002 because the astrometric orbit is well determined and the components, Ba and Bb, are bright enough to be observed at high spectral resolution in the near-IR. Thus, GL 569 B is well suited for the fusion of VB and SB2 techniques to measure the mass of its components. This paper presents our results. We describe our observations and data reduction in §2, the results for GL 569 A and B in §3 and §4, respectively, and discuss our results in §5. We present a summary and suggestions for future work in §6.

2. OBSERVATIONS AND DATA REDUCTION

All observations were obtained at the W. M. Keck Observatory using the facility near-infrared spectrometer NIRSPEC (McLean et al. 2000) and near-IR camera, NIRC-2. We used NIRSPEC in its high spectral resolution mode centered at $1.55 \mu\text{m}$, with and without the adaptive optics (AO) system (Wizinowich et al. 2000). The NIRC-2 observations in the *H*- and *K*-bands were made using AO. Table 1 provides a log of the observations.

We used a 2-pixel wide slit for all NIRSPEC observations which provided spectral resolution $\sim 34,000$ with AO and $\sim 31,000$ without it. With AO, the diffraction resolution was ~ 40 mas. This enabled us to measure the angularly resolved spectra of GL 569 Ba and Bb simultaneously with both objects on the appropriately rotated spectrometer slit. All observations were taken as a series of 240 – 300 s integrations with the targets shifted in an ABBA pattern between two positions separated by $\sim 10''$ on the slit without AO, and

$\sim 1''$ with AO. Sets of 10 flats and 10 darks were median filtered and the results, along with individual AB pairs of target data, were input into the REDSPEC code for rectification, flat-fielding, and spectral extraction¹. The resultant spectra for a single object were then averaged. We worked with NIRSPEC orders 48 and 49, centered at ~ 1.59 and $\sim 1.56\mu\text{m}$, respectively, because these are the most free of telluric absorption of the 9 orders available at the grating setting we used (see Bender et al. 2005, Figure 1). Spectral lamp line integrations were taken to obtain the dispersion solution for the AO spectra. For the non-AO observations, the night sky OH lines were used for this purpose.

We measured radial velocities of the targets with the two-dimensional correlation algorithm TODCOR (Zucker & Mazeh 1994), following procedures we have described previously (e.g., Mazeh et al. 2002). TODCOR requires template spectra for the primary and secondary components. When we observed and reduced NIRSPEC template spectra for the first time (Prato et al. 2002), we compared their radial velocities to similar measurements of the same stars by Duquennoy & Mayor (1991) and Latham (1985) in order to determine the uncertainty, $\pm 1.0 \text{ km s}^{-1}$, in our velocities. More recently, Nidever et al. (2002) have published very precise radial velocities of 844 FGKM stars, including several whose IR spectra we use as templates. We used the Nidever et al. (2002) measurements to correct the velocities of stars earlier than M4 in our suite of templates and used the corrected values to bootstrap improvements to templates of later spectral type. We list the revised values in Table 2; for the stars in common with Prato et al. (2002) all the revised velocities are within 2.2 km s^{-1} of the values given there, and most agree to a few tenths of a km s^{-1} .

The NIRC-2 images have a scale of $0''.00942$ per pixel and a field of view of $\sim 9''.6$, sufficient to include both GL 569 A and B simultaneously. We took data in the H - and K -bands in a five-point dither pattern. Integration times for each frame varied from $0.18 - 1.00 \text{ s}$. After flat-fielding the individual images with the dark-subtracted flat, we expanded the pixel scale by a factor of 10 to improve the measurement precision of the relative positions and photometry for GL 569 A, Ba, and Bb. For the February, 2005 data, we used GL 569 A to centroid the images for shifting and adding multiple exposures and to create an instrumental point-spread function (PSF) in the H - and K -bands. GL 569 A was saturated in the images obtained on December 2004 so we could use these data only for astrometry and relative photometry of GL 569 Ba and Bb.

¹See <http://www2.keck.hawaii.edu/inst/nirspec/redspec/index.html>

3. RESULTS: GL 569 A

The proper motion of GL 569 A is $\mu_\alpha = 275.95$ and $\mu_\delta = -122.12$ mas yr⁻¹ (*HIPPARCOS*). Thus, in the ~ 20 years since the discovery by Forrest et al. (1988) of GL 569 B, the A component has moved $\sim 6''$ on the sky. Our February, 2005 NIRC-2 *H*- and *K*-band images showed the photocenter of GL 569 B $4''.18 \pm 0''.21$ North, and $2''.19 \pm 0''.14$ East with respect to GL 569 A. This offset of B with respect to A lies $\sim 1''$ from that measured by Forrest et al. (1988) (Table 3, Figure 1) and confirms their finding that A and B form a common proper motion system. Our measurement, taken together with the positions measured by Martín et al. (2000) and Lane et al. (2001), clearly indicates the orbital motion of GL 569 B with respect to A (Figure 1).

Using spectroscopy in visible light, Henry & Kirkpatrick (1990) showed that GL 569 A’s spectral type is M2.5 V. To measure the radial velocity of GL 569 A and, in the process, to estimate its spectral type, we analyzed the order 49 spectra obtained on UT 20 April 2003, UT 14 June, 2003, and UT 25 May 2004. The spectrum of the template star GL 436, spectral type M2.5 V (Prato et al. 2002), produced the highest correlation with GL 569 A’s spectrum, in agreement with Henry & Kirkpatrick’s result. The difference between the average of our radial velocity measurements, -7.7 ± 0.6 km s⁻¹ (Table 4), and the center-of-mass velocity of the Ba–Bb pair (§4.3) is 0.8 ± 0.9 km s⁻¹. The velocity difference arising in the orbital motion of B with respect to A is expected to be small (§5) and to lie below the significance limit of our measurements.

The apparent magnitudes of GL 569 A at *V* and *H* are 10.200 ± 0.004 mag and 5.99 ± 0.02 mag, respectively (*HIPPARCOS*, *2MASS*), corresponding to absolute magnitudes $M_V = 10.24$ mag and $M_H = 6.03$ mag at distance 9.81 pc. Using near-IR surface gravity indicators and model stellar spectra, Gorlova et al. (2003) estimated that GL 569 A’s mass is 0.35 ± 0.03 M_⊙. Figure 2 shows M_V and M_H vs mass diagrams using these values. Surprisingly, these mass-luminosity diagrams indicate an age of 20–40 Myr for GL 569 A, much younger than the several hundred Myr estimates of the ages of the brown dwarfs Ba and Bb (Lane et al. 2001; Zapatero Osorio et al. 2004). It is possible, however, that the theoretical isochrones underestimate the age of a star in this range of mass and age (I. Baraffe, priv. comm.). To obtain an independent estimate of the age, we followed K. Luhman’s suggestion (priv. comm. 2005) and placed GL 569 A on a (*V*–*K*) color vs. absolute *K* magnitude diagram (CMD) for the Pleiades cluster, thought to be 100–125 Myr old (Meynet et al. 1993; Stauffer et al. 1998). Figure 3 shows that GL 569 A lies on the Pleiades main-sequence, indicating that it is about the same age. GL 569 A could be older than it appears in Figures 2 or 3 if it were fainter and its apparent magnitude represented that of two stars in a binary. However, its spectrum in both the visible and IR is that of an M 2.5 with no evidence of either a

companion, or variability of its velocity on the three occasions that we measured it in the IR. Its H and K -band images also show no evidence of a companion. We conclude that 1) GL 569 A is a single star, 2) its age is 100-125 Myr, and 3) GL 569 A seems to be younger than the age previously estimated for its brown dwarf companions.

4. RESULTS: GL 569 B

4.1. Photometry, Astrometry, and Orbital Parameters of GL 569 B as a Visual Binary

Figure 4 shows the H - and K -band composite images of GL 569 Ba-Bb from the UT 25 February 2005 NIRC-2 observations. We modeled the brown dwarf binary as the sum of two scaled PSFs; the single star PSF was provided by the simultaneously obtained image of GL 569 A, which had FWHM = 41 mas at H and 53 mas at K . The AO correction achieved a Strehl ratio of ~ 0.3 at H and ~ 0.4 at K . We determined the positions and amplitudes of Ba-Bb relative to each other, and to GL 569 A, by least squares fitting. We used the 2MASS magnitudes of GL 569 A at H and K , 5.99 ± 0.02 mag and 5.77 ± 0.02 mag, respectively, to determine the magnitudes of Ba and Bb. The astrometric and photometric results are given in Table 5. Because we could not use GL 569 A as a PSF (§3) in the December, 2004 data, we formed a composite Ba-Bb PSF by cross-correlating the images and shifting them for greatest correlation. We measured the position of Bb relative to Ba by modeling the PSF as an elliptical Gaussian and fitting to the composite image. The astrometric results and Bb/Ba flux ratios from the December, 2004 observations are included in Table 5. Ba is 0.53 ± 0.08 magnitudes brighter than Bb at K , consistent with the measurement of Lane et al. (2001), and 0.61 ± 0.07 magnitudes brighter at H .

Observations of a VB yield P , a'' , e , i , T_o , ω , and Ω – the orbital period, semi-major axis in arcseconds, eccentricity, inclination, time of periastron passage, longitude of periastron, and longitude of the ascending node, respectively². When the distance to the binary is known, as it is here, the semi-major axis, in physical units, and period determine the total mass of the binary via Kepler’s Third Law. Figure 5 shows the apparent orbit derived from the astrometry reported by Lane et al. (2001), Zapatero Osorio et al. (2004), and Table 5. We calculated the orbital parameters using procedures written by Schaefer (2005) and described in Schaefer et al. (2003). The new values (Table 6) are in excellent agreement

² ω and Ω determined for a VB are degenerate by 180° ; the ambiguity is removed by observation of the system as a spectroscopic binary.

with those published by Zapatero Osorio et al. (2004). Our observations extend the time over which the orbital motion of the GL 569 B binary has been monitored from 0.85 to 2.3 orbital periods; as expected, their main effect is to improve the precision of P and T_o . The total mass of Ba–Bb that follows from these values is $M_{tot} = 0.125 \pm 0.007 M_\odot$. This value is consistent with that determined by Zapatero Osorio et al. (2004) but the uncertainty is larger because our value includes the uncertainty of the *HIPPARCOS* distance measurement and theirs does not.

4.2. Velocities of the GL 569 B Spectroscopic Binary

Non-AO NIRSPEC spectra of GL 569 B do not angularly resolve Ba and Bb. A TOD-COR analysis of blended spectra of GL 569 B using our suite of templates (Table 2) showed that the template spectrum of GL 644 C (M7) provided high correlation. The analysis also showed that precise measurement of the component velocities would be difficult because the radial velocity difference between Ba and Bb is only a few km s^{-1} , the spectra of the components were similar and complex, and the spectral lines of Ba appeared to be significantly broadened. We expected that we would obtain the highest velocity precision by using angularly resolved spectra of Ba and Bb themselves as templates. To this end, we used NIRSPEC with AO to measure their angularly resolved spectra on UT 20 April 2003 and UT 24 May 2004. The small angular separation of Ba and Bb required care in the extraction of their spectra to minimize contamination. Figure 6 illustrates our procedure. The lower panel shows a sample profile of the two-dimensional spectrum in the cross-dispersion direction from UT 24 May 2004, obtained by median filtering a REDSPEC rectified image along the dispersion direction; the AO plate scale is $0''.0182 \text{ pixel}^{-1}$. There is significant blending in the region between Ba and Bb. We modelled the profile as the sum of two Gaussians of equal width with separation equal to that of Ba and Bb. The upper panel of Figure 6 shows the extraction widths, denoted by the vertical lines and hashed regions, chosen to avoid the central region where the profiles are blended. The FWHM of the Gaussians in Figure 6 is about twice the diffraction limit at $1.6\mu\text{m}$. The quality of the seeing and the AO correction varied during the May 2004 observations; the PSF in the profile shown was especially broad. We varied the extraction widths to suit each observation. Figure 6 shows that even in this case the selected regions suffer little contamination. We believe therefore that our procedure produced individual target spectra and hence templates useful for analysis of the blended spectra.

To determine the radial velocity of Ba in orders 48 and 49 on UT 20 April 2003 and UT 24 May 2004, we cross-correlated spectra of Ba with our GL 644 C template, and

found the highest correlation for $v_{rot} \sin i = 25 \text{ km s}^{-1}$, if we interpret the line broadening as attributable to rotation. Similarly, for Bb, using the GL 644 C template, the highest correlation was obtained with $v_{rot} \sin i = 10 \text{ km s}^{-1}$. The measured radial velocities of Ba and Bb in the two orders on the two dates differed by the measurement error. To use the individual Ba and Bb spectra as templates to analyze the blended, non-AO B component spectra, we averaged the measured velocities in orders 48 and 49; these values appear in Table 7.

Figure 7 shows, in the heliocentric reference frame, the April, 2003 and May, 2004 AO resolved spectra of GL 569 Ba and Bb in orders 48 and 49 and, for comparison, a non-AO spectrum of GL 569 B measured on UT 22 February 2005. The spectral range displayed for order 48 is less than that for order 49 because we did not analyze the $\sim 0.007 \mu\text{m}$ wide section shortward of $1.585 \mu\text{m}$ that suffers from terrestrial CO_2 absorption (see Bender et al. 2005, Figure 1). It is evident that the lines in the spectrum of Ba are more broadened than those of Bb. Except for the effects of broadening, the spectral features in Ba and Bb appear identical suggesting that the spectral types must be very similar. These results are consistent with the finding of Zapatero Osorio et al. (2004) that, in their high-resolution, angularly resolved J -band spectra, also obtained using NIRSPEC, Ba and Bb appeared as spectral type M8.5 and M9, with significant broadening characterized by $v_{rot} \sin i \sim 37 \text{ km s}^{-1}$ and 30 km s^{-1} , respectively.

We analyzed the non-AO spectra with TODCOR twice using the two different AO-resolved templates for Ba and Bb from the two different NIRSPEC with AO runs. We list the radial velocities in Table 7. The OH emission lines in order 48 are weaker than those in order 49; on UT 22 December 2002 and UT 14 June 2003, the integration times were not long enough to expose the OH lines for a reliable dispersion solution and we do not list order 48 velocities for those dates. We considered the difference in velocities derived on a given date using the two sets of AO-resolved templates as an empirical measure of the error. Thus, for each order, we considered the differences

$$\Delta_{Ba,i} = V_{Ba,i}(4/03) - V_{Ba,i}(5/04)$$

in which the $V_{Ba,i}$'s are the radial velocities of Ba measured on the i th occasion using the AO templates obtained in April, 2003 and May, 2004 (Table 7). The same procedure was applied to the velocities of Bb. The distribution of the 28 differences is centered at $0.1 \pm 1.7 \text{ km s}^{-1}$, indicating that there is no systematic velocity offset in either set of templates. The standard deviations for the $\Delta_{Ba,i}$ and $\Delta_{Bb,i}$ are 1.8 and 1.4 km s^{-1} , respectively; these values are listed in Table 7 as the velocity uncertainties of the Ba and Bb components. We attribute the larger uncertainty associated with the measurements for Ba to the greater velocity width

of its spectral lines.

4.3. Dynamical Masses of the Components

Velocity measurements of a double-lined spectroscopic binary (SB2) yield $P, e, T_o, \omega, asini$, in physical units, and the velocity semi-amplitudes of the primary and secondary, K_{Ba} and K_{Bb} . These are related to the mass ratio, $q = M_{Bb}/M_{Ba}$, a , and a_{Ba} and a_{Bb} , the semi-major axes of the primary and secondary by $q = K_{Ba}/K_{Bb}$ and $asini = (a_{Ba} + a_{Bb})sini$. $a_{Ba}sini$ is given by

$$a_{Ba}sini = 0.01375K_{Ba}P(1 - e^2)^{1/2}$$

where a_{Ba} is in gigameters, K_{Ba} in km s^{-1} , and P in days. The same result holds for a_{Bb} in terms of K_{Bb} (Heintz 1978).

Here, P, e, i, a'' , and T_o are already known to high precision from the astrometric observations of GL 569 B. In combination with the *HIPPARCOS* distance of GL 569 A, a is known in physical units (Table 6). Our analysis of GL 569 B as an SB2 began by calculating the difference, in the χ^2 sense, of possible velocity solutions to the data, deriving K_{Ba} , K_{Bb} and γ , the center-of-mass velocity, for the minimum value of χ^2 . We did this twice, the first time applying the templates for Ba and Bb measured in April, 2003, and the second using the May, 2004 templates. The minimum reduced χ^2 is ~ 1.1 for both solutions. The results for the velocity semi-amplitude of Bb and the center-of-mass velocity are in excellent agreement with each other, but the results for the velocity semi-amplitude of Ba are not. Using the April, 2003 templates,

$$K_{Ba} = 2.90 \pm 0.50, K_{Bb} = 5.34 \pm 0.50, \gamma = -8.47 \pm 0.30 \text{ km s}^{-1}$$

and using the May, 2004 templates,

$$K_{Ba} = 4.30 \pm 0.70, K_{Bb} = 5.30 \pm 0.50, \gamma = -8.50 \pm 0.30 \text{ km s}^{-1}.$$

We attribute the large difference of the two K_{Ba} values to the large velocity width of Ba's spectrum, as also manifested (§4.2) in the scatter of the $\Delta_{Ba,i}$, larger than that of the $\Delta_{Bb,i}$. Because $K_{Bb} = 5.3 \pm 0.5 \text{ km s}^{-1}$ is well-determined, we analyzed GL 569 B as single-lined system on the basis of the Bb data. Figure 8 shows the velocity vs phase data for the April, 2003 and May, 2004 templates. The velocities of the secondary are fitted with K_{Bb}

and γ as given above. Using the April, 2003 data, the mass function $f(M)$ of the secondary is,

$$f(M) = \frac{(M_{Ba} \sin i)^3}{(M_{Ba} + M_{Bb})^2}$$

$$= 1.036 \times 10^{-7} K_{Bb}^3 P (1 - e^2)^{\frac{3}{2}} M_{\odot}$$

with K in km s^{-1} and P in days (adapted from Heintz 1978). Using $K_{Bb} = 5.3 \pm 0.5 \text{ km s}^{-1}$ and values for P, e, i and $M_{Ba} + M_{Bb}$ from Table 6, we derive that $M_{Ba} = 0.105 \pm 0.011 M_{\odot}$. By subtraction from the total mass, $M_{Bb} = 0.020 \pm 0.013 M_{\odot}$.

The value of M_{Ba} cannot be taken at face value given the similarity of the Ba and Bb spectra (Figure 7) and their flux ratio ~ 0.6 (Table 5). A promising explanation is that Ba itself is a close, angularly unresolved binary, and that GL 569 B consists of three brown dwarfs, two at Ba, one at Bb as previously suggested by Martín et al. (2000) and Kenworthy et al. (2001). The masses of the Ba brown dwarfs are probably $\sim 0.045 - 0.050 M_{\odot}$ each, and that of Bb, $\sim 0.020 - 0.040 M_{\odot}$. This explanation would account for the observed facts: that Ba is about twice as bright as Bb at H, that the total mass is $\sim 0.12 M_{\odot}$, and that the spectra of Ba and Bb appear identical except for the greater line width of Ba. The greater line width of Ba could be attributable either to rotational broadening, which could disguise the presence of an additional component, or some combination of line broadening and Ba orbital motion. If the candidate binary possesses an orbital inclination distinct from and larger than that of the Ba–Bb system, the confusion between broadened lines and velocity shifts would be accentuated, particularly for objects of the similar spectral type. More AO-resolved, high resolution spectra of Ba are required to distinguish among these possibilities.

Figure 9 shows GL 569 Bb on a mass-luminosity (at H) diagram; if its mass at the 1σ upper bound is $0.033 M_{\odot}$, the isochrones indicate a ~ 100 MY age, consistent with that of GL 569 A. We do not know the individual H –magnitudes or masses of the brown dwarfs proposed to comprise GL 569Ba. If their masses are $\sim 0.045 M_{\odot}$ with M_H a few tenths brighter than 11 mag, the isochrones indicate an age > 100 MY. The uncertainties are sufficiently large that it is unclear whether these mass estimates are in conflict.

The derived center-of-mass velocity of Ba–Bb is well determined at $\gamma = -8.50 \pm 0.3 \text{ km s}^{-1}$. It differs, however, by 3 km s^{-1} from the value reported by Zapatero Osorio et al. (2004), $-11.5 \pm 0.5 \text{ km s}^{-1}$. Unlike our measurement, which is referenced to the stellar radial velocities of the spectral type templates, Zapatero Osorio et al. (2004) measured the Doppler shift of the K I doublet in their J -band spectra using the observed and labo-

ratory wavelengths. We believe that our value is representative of the actual value because it is based on all the lines in the spectra. Our measurement thus avoids the complications of measuring a Doppler shift of the pressure broadened and nearly saturated lines of the K I doublet. Moreover, for M spectral types, contamination by Mg I at $1.24369 \mu\text{m}$ and particularly by Cr I at $1.25253 \mu\text{m}$ for later types can shift the line centers of the K I doublet at $1.24356 \mu\text{m}$ and $1.25255 \mu\text{m}$. The fact that our measured center-of-mass velocity differs from the radial velocity of GL 569 A by only $0.8 \pm 0.9 \text{ km s}^{-1}$ also suggests that it is close to the actual value. The $\sim 3 \text{ km s}^{-1}$ difference between our value and that of Zapatero Osorio et al. (2004) affects only their absolute radial velocities. The differences in the radial velocities of Ba and Bb measured by Zapatero Osorio et al. (2004) (their Table 4 and Figure 8) agree well with the differences derived from our values in Table 7, as shown in our Figure 10.

5. DISCUSSION

5.1. The GL 569 Quadruple?

Our work suggests that GL 569 may be a quadruple consisting of an M2.5 V star (GL 569 A) accompanied by three nearly equal mass brown dwarfs and distributed as follows:

- 1) The wide binary, GL 569 A – GL 569 B, at separation $\sim 5''$ ($\sim 50 \text{ AU}$) with total mass $(0.35 \pm 0.03 + 0.125 \pm 0.007) = 0.48 \pm 0.03 M_{\odot}$. If it is oriented face-on, its orbital period is $\sim 500 \text{ yrs}$.
- 2) The binary GL 569 Ba – GL 569 Bb which has semi-major axis 90 mas (0.89 AU), period 864 days , and total mass $0.125 \pm 0.007 M_{\odot}$. Bb is a single brown dwarf with mass $0.020 \pm 0.013 M_{\odot}$.
- 3) Ba is a candidate unresolved inner brown dwarf binary with total mass $0.105 \pm 0.011 M_{\odot}$.

Designating the two components of Ba, the inner binary, as Baa and Bab, we consider the limits that can be placed on their orbit empirically by our spectroscopic and imaging observations, and theoretically by the requirement that Ba and Bb form a stable triple. By simulating the inner binary as composed of two equal brightness brown dwarfs of late M spectral type, rotationally broadened to 10 km s^{-1} , we found that we could measure their individual velocities reliably to $\sim 5 \text{ km s}^{-1}$. We measured no significant velocity differences in the two AO spectra of Ba. We conclude that the observed velocity difference of the two components was $\leq 5 \text{ km s}^{-1}$ at the times of the observations if the components had $\sim 10 \text{ km s}^{-1}$ rotational broadening. With $M_{\text{tot}} = 0.105 M_{\odot}$, this implies that the semi-major axis of the inner binary satisfies $a_{\text{inner}} \gtrsim 3.8 \sin^2 i_{\text{inner}} \text{ AU}$, where i_{inner} is the inclination of the

inner binary.

The FWHM of the H-band PSF was 41 mas in the images obtained on UT 25 February 2005. We analyzed images of model binaries with equal brightness components convolved with the PSF and the same signal to noise as the H-band image in Figure 4. We were able to identify the two components at separations as small as ~ 10 mas. The actual situation is complicated by the presence of the third component, Bb, at apparent separation ~ 85 mas (Table 5), $2 \times \text{FWHM}$ of the PSF. It is apparent in Figure 4 that the broad wings of the PSF extend from Bb to Ba. We estimate that Baa and Bab would have to lie at apparent separation $\gtrsim 20$ mas for their presence to be recognizable in our images. This limit, combined with that from the spectroscopic observations, restricts i_{inner} to $\lesssim \pm 13.6^\circ$.

Theoretical study of the stability of triples has an extensive literature and continues to be an interesting area of research as new environments are identified (e.g., the formation of planets in stellar binaries, Holman & Weigert 1999) and the meaning of “stability” is sharpened (e.g., Ford et al 2000). Eggleton & Kiseleva (1995) presented an empirical stability criterion in terms of Y^{min} , the ratio of the periastron distance of the outer binary to the apastron distance of the inner binary,

$$Y^{\text{min}} = \frac{a_{\text{outer}}(1 - e_{\text{outer}})}{a_{\text{inner}}(1 + e_{\text{inner}})}$$

When values of Y^{min} larger than a critical value Y_0^{min} are realized, the triple is stable. The criterion is applicable to triples with various inclinations, eccentricities, and relative phases of the inner and outer binaries. For a triple with equal mass components (see Eggleton & Kiseleva 1995, eqn. 2), $Y_0^{\text{min}} \sim 5$. With $a_{\text{outer}} = 0.90$ AU and $e_{\text{outer}} = 0.31$ (Table 6), $a_{\text{inner}}(1 + e_{\text{inner}}) = 0.13$ AU; $a_{\text{inner}} = 0.13$ AU if $e_{\text{inner}} = 0$, and 0.07 AU if $e_{\text{inner}} = 0.9$. In the latter case, the apastron of the inner binary is 0.13 AU. We conclude that the largest value of a_{inner} for stability, 0.13 AU, is consistent with our observational limits if i_{inner} lies in the range $\pm 11^\circ$.

5.2. The Lithium Test

The Li spectral line at 6708 Å is a sensitive mass and age indicator because brown dwarfs with mass $> 0.06 M_\odot$ destroy their Li within a few hundred Myr (Magazzù et al. 1993; Chabrier & Baraffe 2000). The masses we have estimated for Baa, Bab, and Bb are at this boundary. In spectroscopic observations that did not resolve the GL 569 B system, Magazzù et al. (1993) did not detect the Li line, suggesting that the brown dwarf masses

are greater than the values we infer. Detection of the Li feature in GL 569 B may have been frustrated by the large line widths revealed by our analysis of the IR spectra and the possible triple nature of the system.

6. Summary and Suggestions for Future Work

There are two main results of our work:

1) The previous suggestions that Ba could be a binary brown dwarf were based on the fact that Ba is ~ 1.6 times brighter than Bb in the near IR and that the near IR colors of the two are similar (Martín et al. 2000; Kenworthy et al. 2001). Our work confirms these observations and strengthens the case for the binarity of Ba in three respects: *i)* the finding that $M_{Ba} = 0.105 \pm 0.011 M_{\odot}$ and Ba cannot be a star of this mass, *ii)* the similar spectra of Ba and Bb indicate that Ba and Bb contain similar brown dwarfs, and *iii)* the greater width of the lines of Ba, $\sim 25 \text{ km s}^{-1}$, than that of Bb, $\sim 10 \text{ km s}^{-1}$, has a natural explanation if Ba harbors two brown dwarfs.

These arguments and the total mass of the system $M_{tot} = 0.125 \pm 0.007 M_{\odot}$ also suggest that the masses of the three components Baa, Bab, and Bb, are approximately equal and in the range 0.04 to 0.05 M_{\odot} .

2) The location of GL 569 A with respect to theoretical isochrones and in the Pleiades CMD, and the location of Bb with respect to theoretical isochrones (and also of Baa and Bab if they have approximately equal mass) indicate that the age the GL 569 system is 100-125 Myr.

The GL 569 quadruple is well suited to improve our understanding of objects at the low mass end of the IMF. We suggest the following observations to confirm and advance beyond the results we have presented.

A) Detection of the Li line in the spectra of GL 569 Ba and Bb both would confirm the mass of GL 569 Bb and that Ba must be composed of two brown dwarfs. The spectroscopic measurement should resolve Ba and Bb to avoid the complications of interpreting the complex spectrum of three unresolved brown dwarfs. This would require AO-assisted spectroscopic observations in the visible, a capability not yet available.

B) Additional high angular resolution IR spectroscopy of Bb will improve the precision of the velocity semi-amplitude K_{Bb} , and hence of M_{Ba} and M_{Bb} .

C) High angular resolution IR spectroscopy of Ba may distinguish the two brown dwarfs Baa

and Bab, and hence determine their parameters as a double-lined spectroscopic binary.

D) At separation ~ 7 mas, the inner binary is resolvable by the present generation of IR interferometers and is not far below their present sensitivity limits. The VB parameters of the inner binary, combined with the SB2 parameters would determine the individual masses M_{Baa} and M_{Bab} and reveal whether the orbits in the hierarchical triple are coplanar.

Of the observations suggested only the AO-resolved IR spectroscopic observations B and C are possible now. We plan to continue with these and look forward to the technical advances that will enable the interferometric and visible light spectroscopic studies.

We acknowledge with pleasure I. Baraffe, L. Close, J. Lissauer, K. Luhman, and J. Stauffer for their helpful advice and thank K. Luhman for providing us with the Pleiades data used in Figure 3. We thank G. Schaefer for use of her computer programs for the analysis of astrometric orbits and S. Zucker and T. Mazeh for the use of their TODCOR program for the measurement of velocities in blended spectra. We are grateful to A. Tokunaga for collaborating on initial observations at the Subaru telescope. We thank the Keck Observatory OAs and staff for their expert assistance. This research was supported in part by NSF Grant 02-05427 to MS and NSF Grant 04-44017 to LP. LP also acknowledges support from Keck PI Data Analysis funds, administered by JPL for Keck time allocated through NASA. The authors benefitted from time allocations through the NOAO-administered NSF TSIP program. Data presented herein were obtained at the W. M. Keck Observatory, which is operated as a scientific partnership between the California Institute of Technology, the University of California, and NASA. The Observatory was made possible by the generous financial support of the W. M. Keck Foundation. The authors wish to extend special thanks to those of Hawaiian ancestry on whose sacred mountain we are privileged to be guests. Our research used the SIMBAD database, operated at CDS, Strasbourg, France and data products of 2MASS, which is a joint project of the Univ. of Massachusetts and IPAC at the California Institute of Technology, funded by NASA and NSF.

REFERENCES

- Baraffe, I., Chabrier, G., Barman, T. S., Allard, F., & Hauschildt, P. H. 2003, *A&A*, 402, 701
- Baraffe, I., Chabrier, G., Allard, F., & Hauschildt, P. H. 1998, *A&A*, 337, 403
- Bender, C., Simon, M., Prato, L., Mazeh, T., & Zucker, S. 2005, *AJ*, 129, 402

- Bouy, H., et al. 2004, A&A, 423, 341
- Burgasser, A. J., Kirkpatrick, J. D., & Lowrance, P. J. 2005, AJ, 129, 2849
- Burrows, A., et al. 1997, ApJ, 491, 856
- Chabrier, G., & Baraffe, I. 2000, ARA&A, 38, 337
- Duquennoy, A., & Mayor, M. 1991, A&A, 248, 485
- Eggleton, P. & Kiseleva, L. 1995, ApJ, 455, 640
- Ford, E.B., Kozinsky, B., and Rasio, F.A. 2000, ApJ, 535, 385
- Forrest, W. J., Skrutskie, M. F., & Shure, M. 1988, ApJ, 330, L119
- Gorlova, N. I., Meyer, M. R., Rieke, G. H., & Liebert, J. 2003, ApJ, 593, 1074
- Henry, T. J., & Kirkpatrick, J. D. 1990, ApJ, 354, L29
- Heintz, W. D. 1978, Double Stars (Boston,MA:D.Reidel)
- Holman, M.J. & Wiegert, P.A. 1999, AJ, 117, 621
- Kenworthy, M., et al. 2001, ApJ, 554, L67
- Lane, B. F., Zapatero Osorio, M. R., Britton, M. C., Martín, E. L., & Kulkarni, S. R. 2001, ApJ, 560, 390
- Latham, D. W. 1985 in IAU Colloq. 85, *Stellar Radial Velocities*, eds. A. G. D. Philip & D. W. Latham (Schenectady:L.Davis Press), 5
- Luhman, K. L., Stauffer, J. R., & Mamajek, E. E. 2005, ApJ, 628, L69
- Magazzù, A, Martín, E.L, & Rebolo, R., 1993, ApJ, 404, L17
- Martín, E. L., Koresko, C. D., Kulkarni, S. R., Lane, B. F., & Wizinowich, P. L. 2000, ApJ, 529, L37
- Mazeh, T., Prato, L., Simon, M., Goldberg, E., Norman, D., & Zucker, S. 2002, ApJ, 564, 1007
- McLean, I. S., Graham, J. R., Becklin, E. E., Figer, D. F., Larkin, J. E., Levenson, N. A., & Teplitz, H. I. 2000, Proc. SPIE, 4008, 1048.
- Meynet, G., Mermilliod, J. -C., & Maeder, A. 1993, A&AS, 98, 477

- Nidever, D. L., Marcy, G. W., Butler, R. P., Fischer, D. A., & Vogt, S. S. 2002, *ApJS*, 141, 503
- Prato, L., Simon, M., Mazeh, T., McLean, I. S., Norman, D., & Zucker, S. 2002, *ApJ*, 569, 863
- Pravdo, S. H., Shaklan, S. B., & Lloyd, J. 2005, *ApJ*, 630, 528
- Schaefer, G. H., Simon, M., Nelan, E., & Holfeltz, S. T. 2003, *AJ*, 126, 1971
- Schaefer, G. H. 2005, PhD Thesis, SUNY-Stony Brook
- Stassun, K. G., Mathieu, R. D., Vaz, L. P. R., Valenti, J. A., & Gomez, Y. 2005, in *LPI Contribution No. 1286, Protostars and Planets V*, 8628
- Stauffer, J. R., Schultz, G. & Kirkpatrick, J. D. 1998, *ApJS*, 499, 199
- Wizinowich, P., Acton, D. S., Lai, O., Gathright, J., Lupton, W., & Stomski, P. J. 2000, *Proc. SPIE*, 4007, 64
- Zapatero Osorio, M. R., Lane, B. F., Pavlenko, Y., Martín, E. L., Britton, M., & Kulkarni, S. R. 2004, *ApJ*, 615, 958
- Zucker, S., & Mazeh, T. 1994, *ApJ*, 420, 806

Table 1. Log of Observations

UT Date	MJD	Instrument	Mode	Targets
2002 Jul 18	52473.3	NIRSPEC	non-AO	GL569B
2002 Dec 22	52630.7	NIRSPEC	non-AO	GL569B
2003 Mar 25	52723.5	NIRSPEC	non-AO	GL569B
2003 Apr 20	52749.4	NIRSPEC	AO	GL569A, GL569Bab
2003 Jun 14	52804.2	NIRSPEC	non-AO	GL569A, GL569B
2004 Jan 26	53030.6	NIRSPEC	non-AO	GL569B
2004 Apr 29	53124.4	NIRSPEC	non-AO	GL569B
2004 May 24	53149.3	NIRSPEC	AO	GL569Bab
2004 May 25	53150.3	NIRSPEC	AO	GL569A
2004 Dec 24	53363.7	NIRC2	AO	GL569Bab
2004 Dec 26	53365.7	NIRSPEC	non-AO	GL569B
2005 Feb 22	53423.5	NIRSPEC	non-AO	GL569B
2005 Feb 25	53426.5	NIRC2	AO	GL569A, GL569Bab

Table 2. Revised Template Library Radial Velocities

Star	Sp. Type	Obs. Date	V_{rad} (km s ⁻¹)
GL15A	M1.5	2000 Jun 10	11.81
GL436	M2.5	2001 Jan 5	9.61
GL752A	M3	2000 Jun 9	35.88
GL213	M4	2000 Jan 8	105.96
GL402	M4	2001 Jan 5	-1.04
GL669B	M4.5	2000 Jun 10	-34.90
GL406	M5.5	2001 Jan 5	18.61
LHS292 ^a	M6.5	2001 Jan 5	1.35
GL644C	M7	2001 Feb 2	15.21
LHS2351	M7	2001 Feb 2	0.72
LHS2065 ^b	M9	2001 Feb 2	7.02
2MASS 0208+25	L1	2002 Dec 15	20.79

^aReported to be a spectroscopic binary; ^bX-ray flare star
(Guenther & Wuchterl 2003)

Table 3. Astrometry of GL 569 AB

Date	R.A. $\times \cos(\text{Dec})$ (")	Dec (")	Reference
1985.6	1.52 ± 0.15	4.84 ± 0.15	Forrest, Skrutskie, & Shure (1988)
1999.7	2.11 ± 0.08	4.53 ± 0.04	Martín et al. (2000)
2001.1	2.45 ± 0.22	4.23 ± 0.13	Lane et al. (2001)
2005.2	2.72 ± 0.14	4.18 ± 0.21	this work

Table 4. Radial Velocity Measurements of GL 569 A

MJD	V_{rad} (km s $^{-1}$)
52749.4	-7.1 \pm 1.0
52804.3	-8.1 \pm 1.0
53150.3	-7.8 \pm 1.0
Average	-7.7 \pm 0.6

Table 5. Photometry and Astrometry of GL 569 B

MJD	Exp. (s)	H _{Ba}	H _{Bb}	K _{Ba}	K _{Bb}	Δm_H	Δm_K	Sep. (″)	P. A. (°)
53363.7	100	0.61 \pm 0.03	...	0.0885 \pm 0.0048	111.3 \pm 1.2
53426.5	22	10.43 \pm 0.04	11.04 \pm 0.05	9.86 \pm 0.05	10.39 \pm 0.06	0.57 \pm 0.04	0.61 \pm 0.04	0.0798 \pm 0.0029	133.7 \pm 0.7

Table 6. Orbital Parameters of GL 569 Bab

Parameter	Visual Binary Orbit	
	Zapatero Osorio et al. (2004)	This Work
P (days)	876 \pm 9	863.7 \pm 4.2
T (MJD, days)	51, 822 \pm 3	51820.9 \pm 2.6
e	0.32 \pm 0.01	0.312 \pm 0.007
a (mas)		90.4 \pm 0.7
a (AU)	0.90 \pm 0.01 ^a	0.89 \pm 0.02 ^b
i (deg)	34 \pm 2	32.4 \pm 1.3
ω (deg)	257 \pm 2	256.7 \pm 1.7
Ω (deg)	321.5 \pm 2.0	321.3 \pm 2.2
M_{total} (M $_{\odot}$)	0.125 \pm 0.005 ^a	0.125 \pm 0.007 ^b

^aDoes not include 1.6% parallax uncertainty; ^bdoes include 1.6% parallax uncertainty

Table 7. Radial Velocity Measurements of GL 569 Bab

MJD	phase	V_{rad} (km s ⁻¹)			
		GL 569 Ba		GL 569 Bb	
		Order 49	Order 48	Order 49	Order 48
GL644C Templates					
52749.4	0.072	-7.92±0.90		-9.98±0.90	
53149.3	0.535	-8.50±0.90		-8.38±0.90	
April 20, 2003 Templates					
52473.3	0.753	-10.89±1.80	-11.60±1.80	-4.71±1.40	-3.19±1.40
52630.7	0.935	-11.60±1.80	...	-3.65±1.40	...
52723.5	0.042	-9.46±1.80	-7.12±1.80	-8.07±1.40	-7.74±1.40
52804.2	0.136	-7.21±1.80	...	-14.15±1.40	...
53030.6	0.397	-7.52±1.80	-4.92±1.80	-12.72±1.40	-11.74±1.40
53124.4	0.506	-9.07±1.80	-8.54±1.80	-9.56±1.40	-7.29±1.40
53365.7	0.785	-10.62±1.80	-12.31±1.80	-4.98±1.40	-3.09±1.40
53423.5	0.852	-10.75±1.80	-11.71±1.80	-3.99±1.40	-1.98±1.40
May 24, 2004 Templates					
52473.3	0.753	-12.30±1.80	-10.93±1.80	-4.57±1.40	-3.38±1.40
52630.7	0.935	-12.12±1.80	...	-3.96±1.40	...
52723.5	0.042	-6.92±1.80	-4.54±1.80	-10.28±1.40	-9.98±1.40
52804.2	0.136	-6.29±1.80	...	-13.21±1.40	...
53030.6	0.397	-5.42±1.80	-4.49±1.80	-13.03±1.40	-11.28±1.40
53124.4	0.506	-6.96±1.80	-5.34±1.80	-11.64±1.40	-11.14±1.40
53365.7	0.785	-12.90±1.80	-12.66±1.80	-4.40±1.40	-3.75±1.40
53423.5	0.852	-12.76±1.80	-11.82±1.80	-3.41±1.40	-2.70±1.40

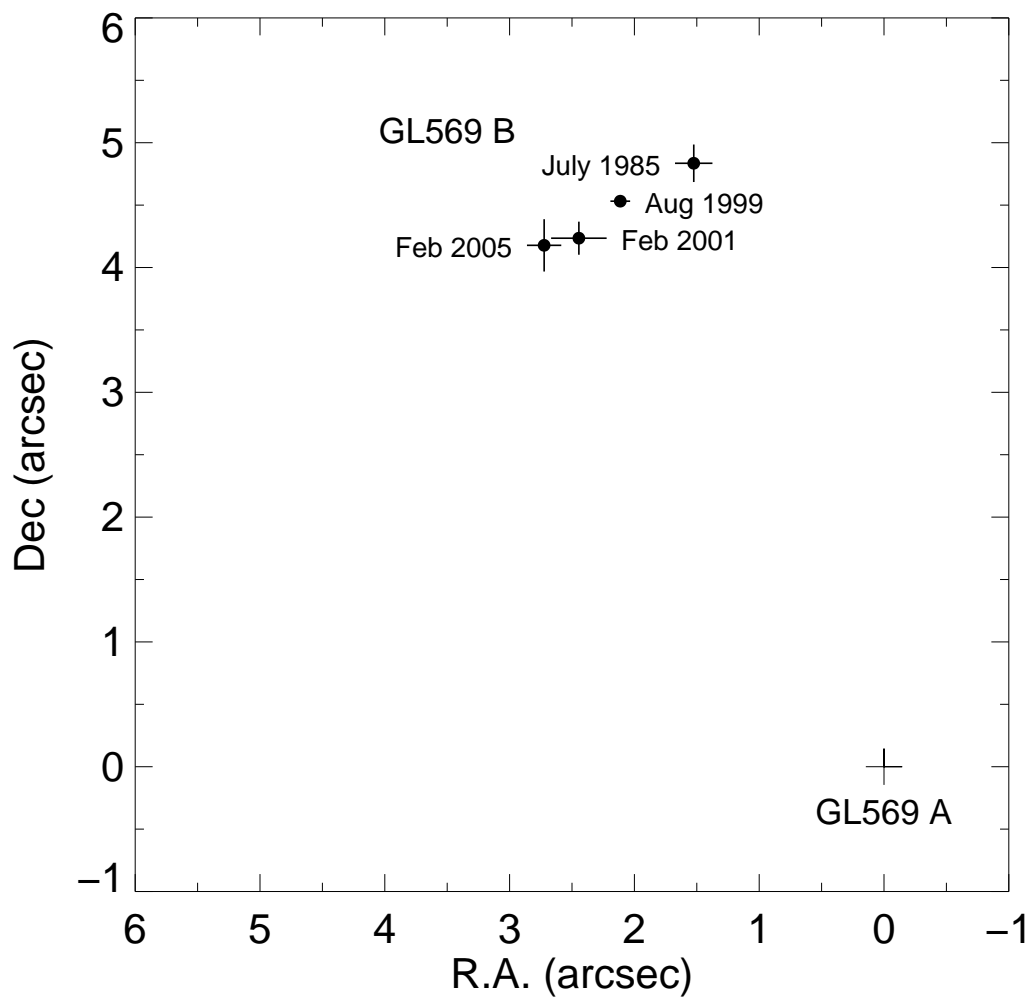


Fig. 1.— The position of GL 569 B with respect to A using our measurement and the earlier measurements listed in Table 3. A and B form a common proper motion system (see §3); the figure shows orbital motion of B with respect to A. North is up and east is to the left.

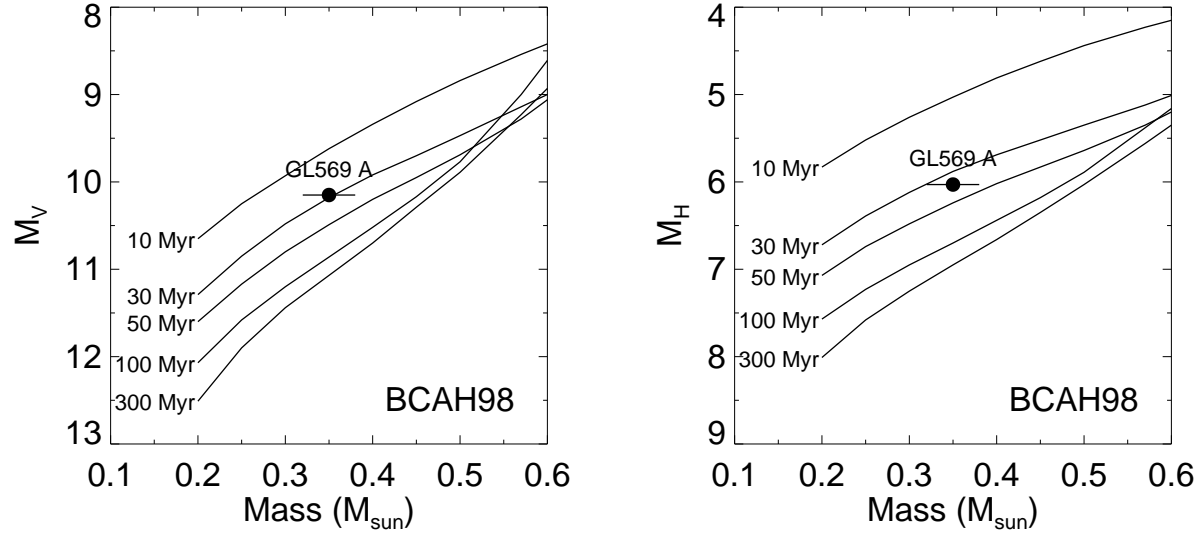


Fig. 2.— Absolute V and H magnitudes and mass of GL 569 A compared to theoretical isochrones calculated by Baraffe et al. (1998).

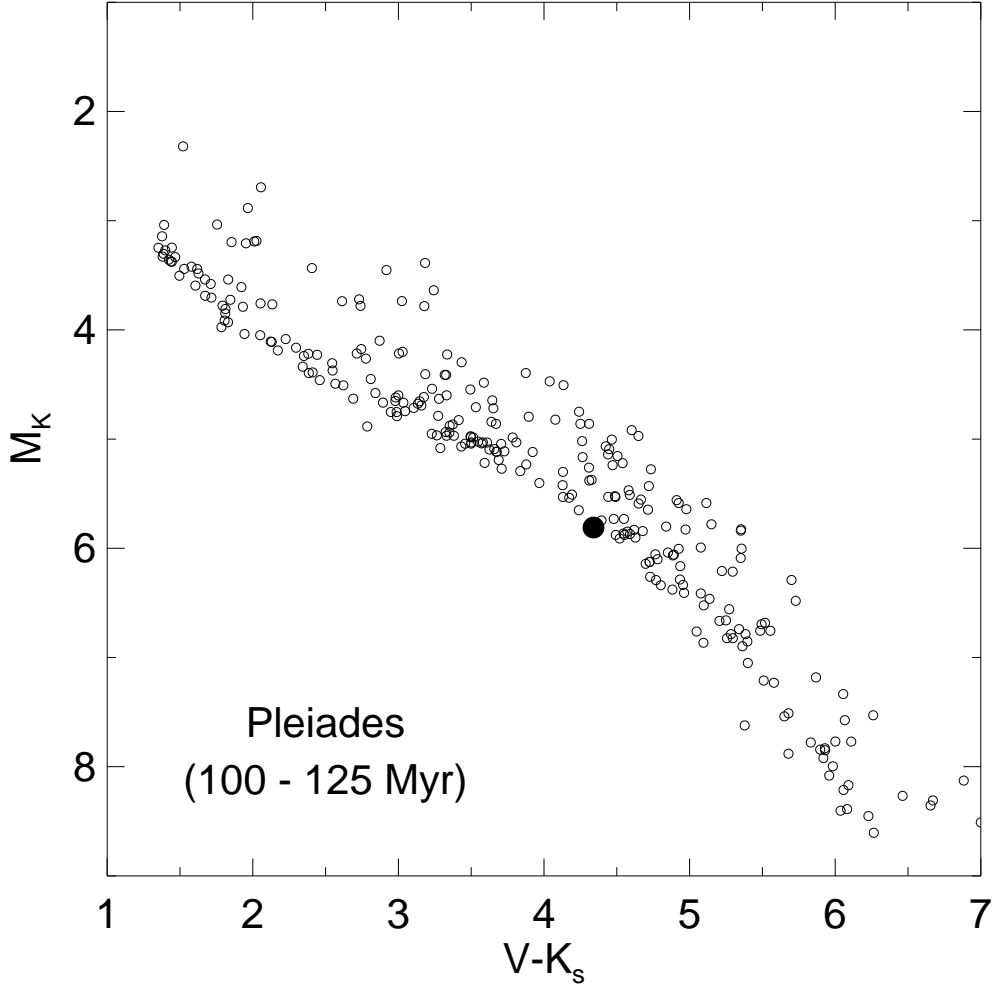


Fig. 3.— Absolute K mag and $V-K$ color of GL 569 A (filled circle) on a color-magnitude diagram of the Pleiades. The Pleiades data is the same as in Luhman et al. (2005) Figure 1, and is for an adopted extinction $A_V = 0.12$ mag and distance 133 pc for the Pleiades.

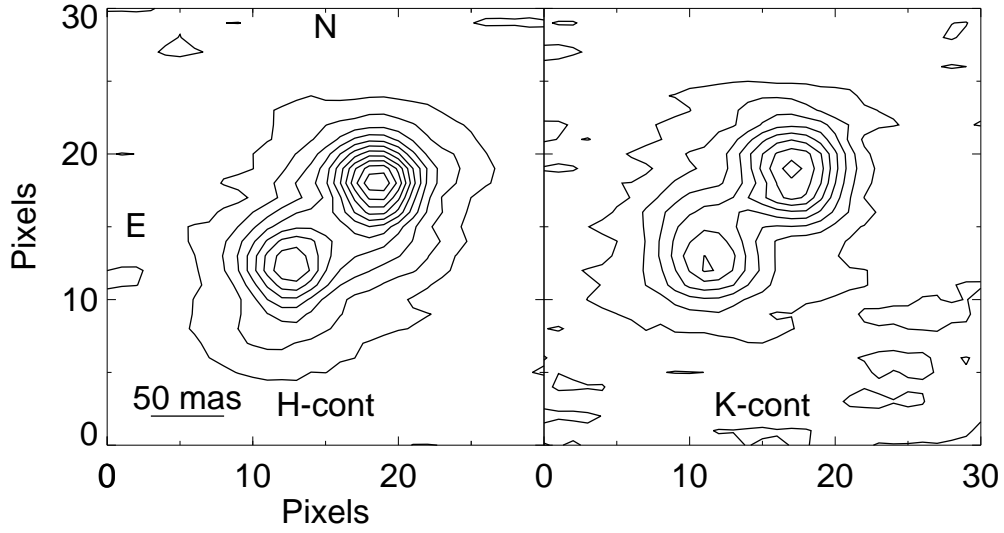


Fig. 4.— NIRC-2 adaptive optics images of GL 569 Ba and Bb at H and K obtained on UT 25 February 2005. North is up and east is to the left. The images show a subsection of the frame; GL569 A was imaged in the same field, but is not shown. The first contour represents 1000 counts, $\sim 5\sigma$ over the background noise, and each subsequent contour is an additional 1000 counts. Ba is located northwest of Bb and is clearly the brighter component; the Bb/Ba flux ratios are 0.57 ± 0.04 and 0.61 ± 0.04 in H and K respectively.

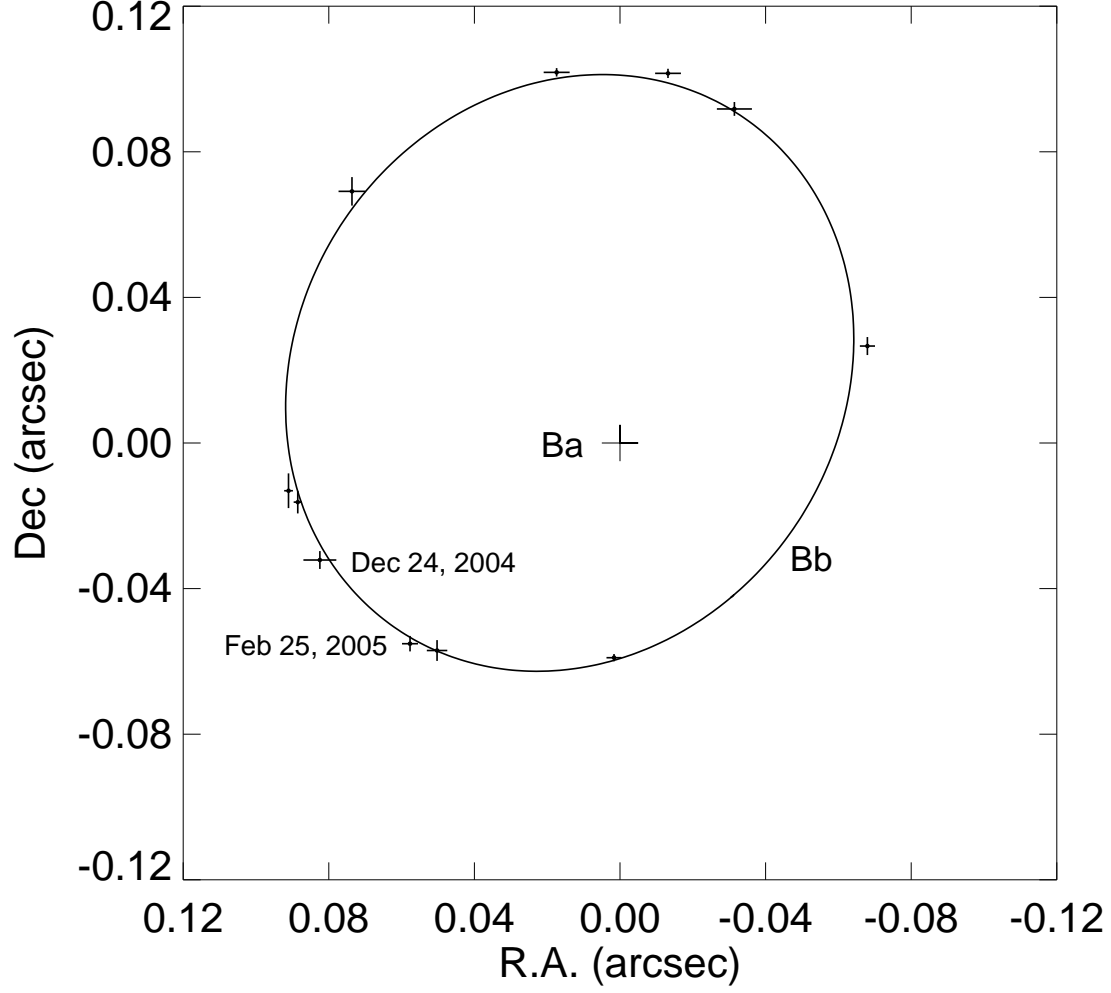


Fig. 5.— The astrometric orbit of GL 569 Bb with respect to Ba at the coordinate origin, using our measurements from UT 24 December 2004 and UT 25 February 2005 together with the earlier measurements given in Zapatero Osorio et al. (2004). The best fit orbit corresponds to our updated parameters in Table 6.

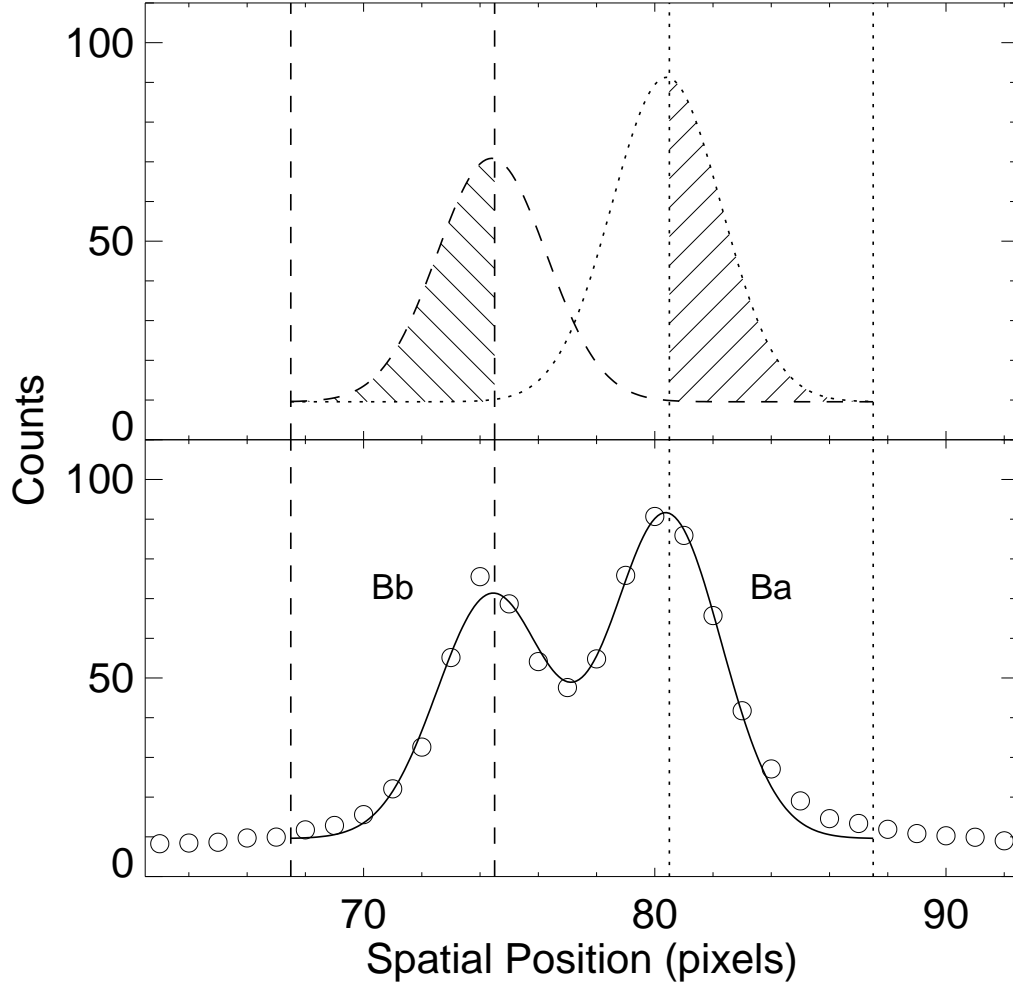


Fig. 6.— A sample profile in the cross-dispersion direction of the AO angularly resolved Order 49 GL569 Ba and Bb two-dimensional spectrum from UT 24 May 2004. The open circles (bottom panel) show the measured spatial profile of the resolved spectra; the solid line is a least squares fit of two Gaussians with equal widths (see text). The dotted and dashed curves (top panel) are the individual Gaussian profiles. The vertical lines and hashed areas indicate the spatial regions used to extract each spectrum.

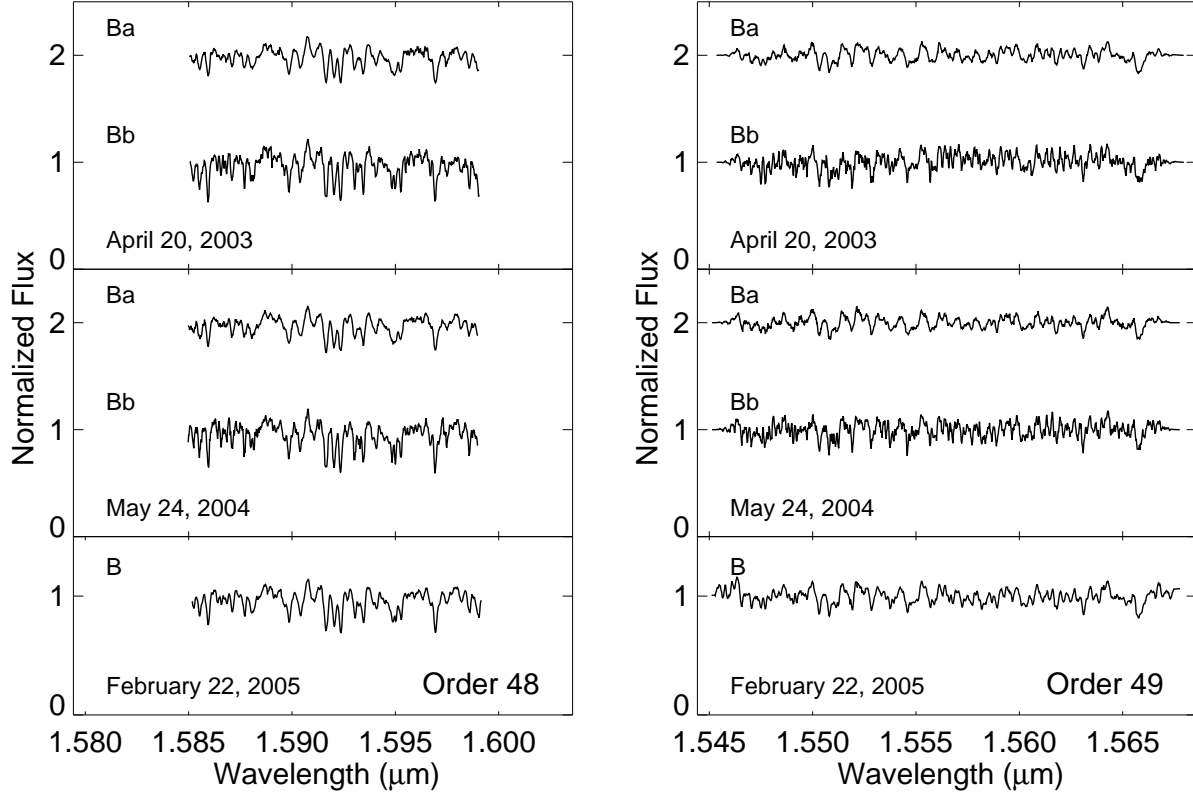


Fig. 7.— Angularly resolved spectra of GL 569 Ba and Bb measured on UT 20 April 2003 and UT 24 May 2004, compared with a spectrum measured on UT 22 February 2005 in which Ba and Bb are unresolved. NIRSPEC spectral orders 48 (left) and 49 (right) are shown. The wavelength span of the order 48 spectra is about 2/3 that of the order 49 spectra because the $\sim 0.007 \mu\text{m}$ wide section shortward of $1.585 \mu\text{m}$ is contaminated by a terrestrial CO_2 band and not shown. The spectra are normalized to 1 in the continuum and are plotted on a 0 to 1 flux scale with the Ba spectra in the top two panels offset by +1 in flux.

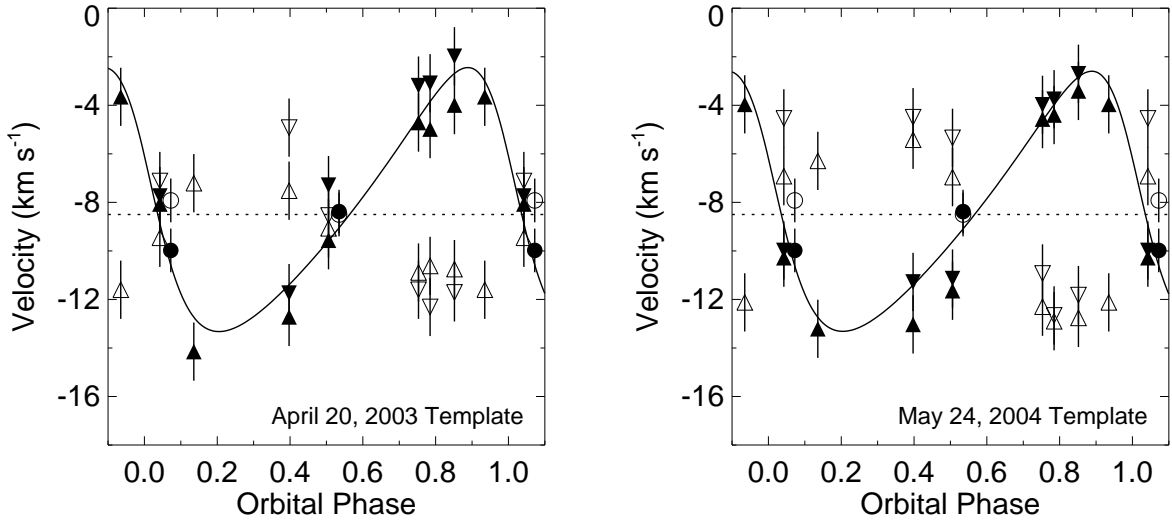


Fig. 8.— Velocity *vs* orbital phase measurements for GL 569 Ba (open triangles) and Bb (filled triangles) using the UT 20 April 2003 templates (left) and UT 24 May 2004 templates (right). Order 48 and 49 data are plotted as downward and upward pointing triangles, respectively. The measurements obtained with AO, averaged over orders 48 and 49, are indicated with open (Ba) and filled (Bb) circles. The dashed line is the fitted center-of-mass velocity, -8.5 km s^{-1} , and the solid line is the model fit with $K_{Bb} = 5.3 \text{ km s}^{-1}$ and P, e, i , and ω given in Table 6.

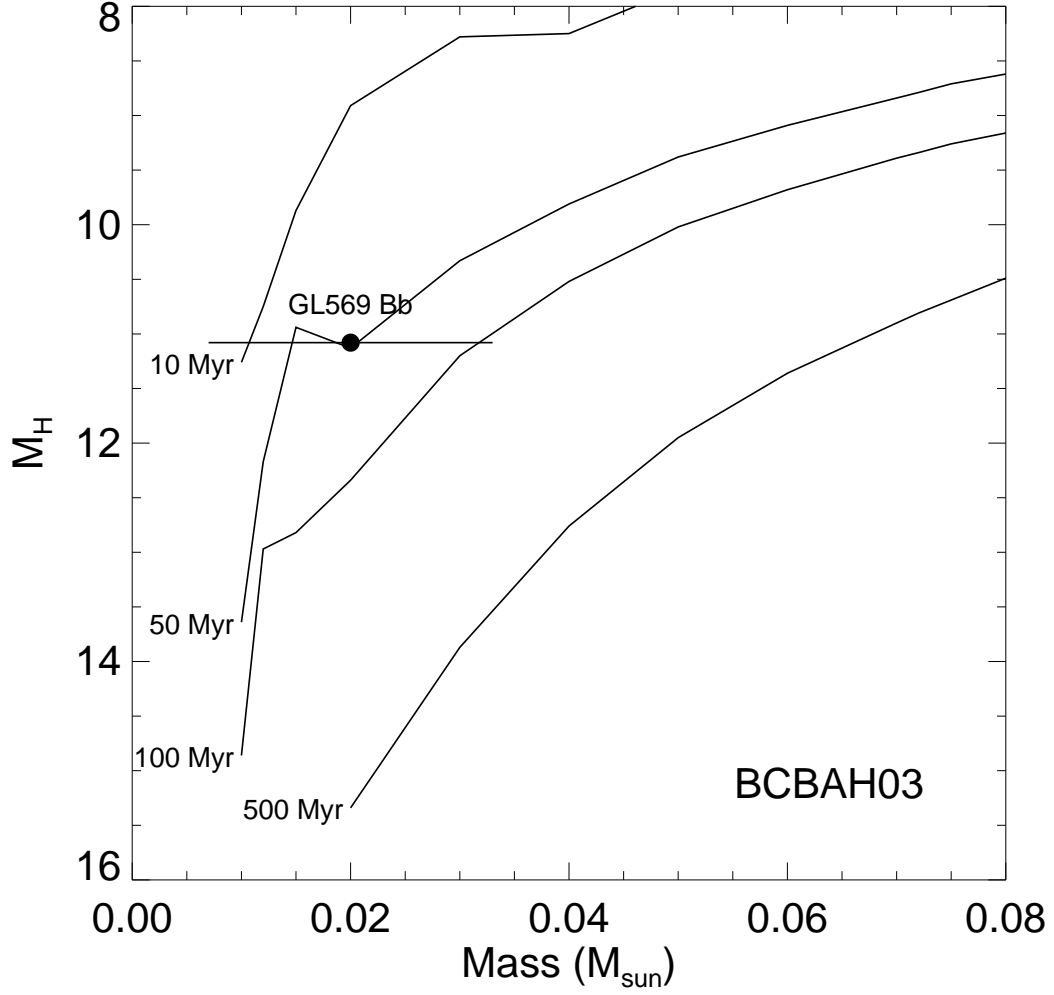


Fig. 9.— GL 569 Bb with $M_H = 11.08 \pm 0.05$ mag and mass $0.020 \pm 0.013 M_{\odot}$ compared with theoretical isochrones calculated by Baraffe et al. (2003). Its location is consistent with an age of ~ 100 Myr.

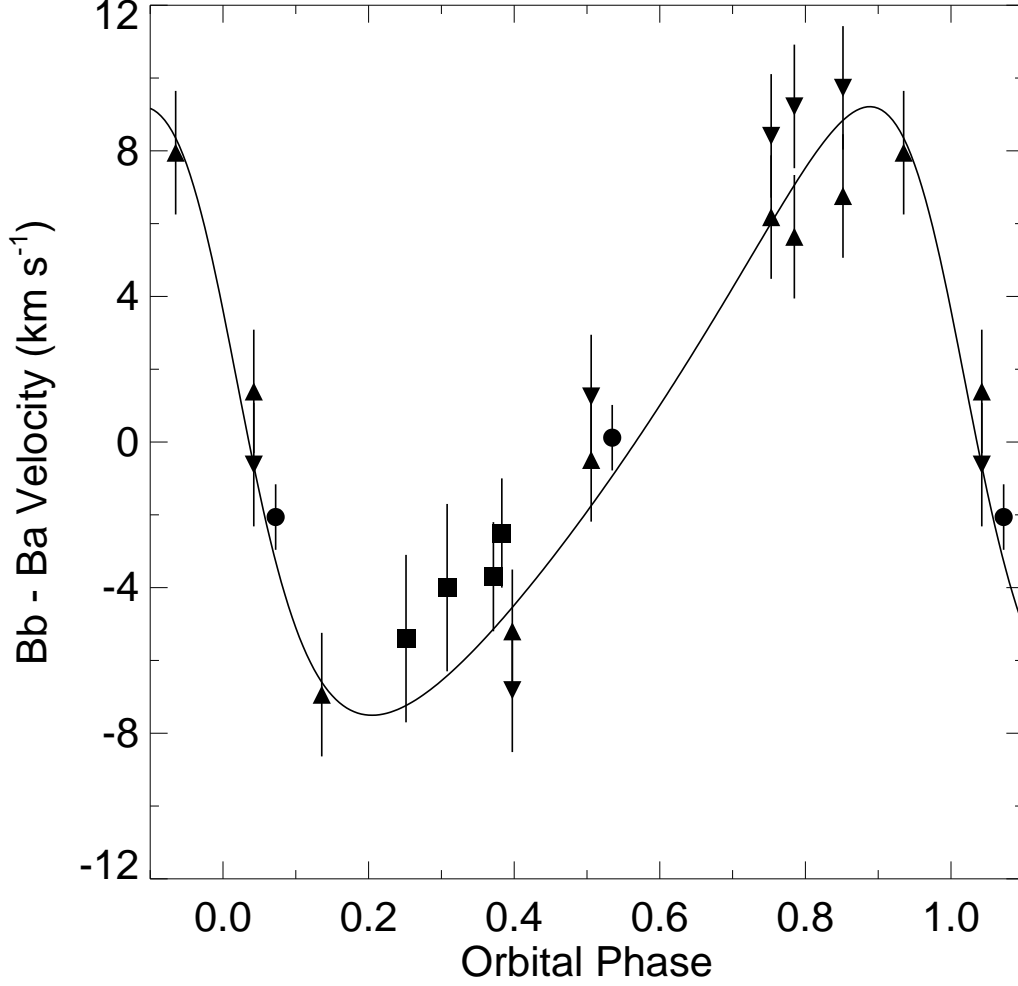


Fig. 10.— Differences of the GL 569 Ba and Bb velocities *vs* orbital phase using our measurements in Table 7 with the UT 20 April 2003 templates for: order 48 (downward triangles), order 49 (upward triangles), and AO (circles). Our data are consistent with the values (squares) reported by Zapatero Osorio et al. (2004).